Liquefaction potential hazard study at UIN Datokarama, Palu City, Central Sulawesi

Azmi Mulki[1*], *Ahmad* Rifa'i[1], and *Sito* Ismanti[1]

[1]Master in Engineering in Natural Disaster Management, Universitas Gadjah Mada, Bulaksumur, Yogyakarta, Indonesia

Abstract. In June 2019, the Asian Development Bank approved emergency rehabilitation and reconstruction assistance (EARR) to help Indonesia rebuild better critical infrastructure damaged by the 2018 Palu-Donggala earthquake. One of the EARR sub-projects is the reconstruction of Universitas Islam Negeri (UIN) Datokarama that suffered significant damage from the combined effects of the tsunami and earthquake. The design for the building's reconstruction incorporated better principles of deconstruction, including pile foundations to ensure the facilities are earthquake, tsunami, and liquefaction resistant. This study purpose is to evaluate liquefaction potential and estimate its severity or damage potential to structures in the reconstruction site. Liquefaction potential will be assessed in two ways, first by using soil deposits grain sizes distribution method from Japan technical standards for port and harbour facilities and second by safety factor against liquefaction (FOS) method using the SPT-based liquefaction triggering analysis with the revised magnitude scaling factor (MSF) relationship by Idriss and Boulanger. Liquefaction Potential Index (LPI) from Iwasaki will be used for estimating liquefaction severity. The analysis is performed on dataset taken from 6 boreholes in location dominated by saturated sandy soil and shallow ground water. Based on the result, liquefaction potentially triggered at various depth with consistent LPI index at > 15, The reconstruction site has a very high liquefaction risk.

1 Introduction

On September 28, 2018, Earthquake with a magnitude of 7.5 in Palu-Donggala that resulted in considerable destruction in the Central Sulawesi area of Indonesia, particularly in Palu City. The earthquake triggered a sequence of disastrous flowslides, building collapses, and produced tsunami waves that crushed Palu Bay's coastline. The site of UIN Datokarama - Campus I is located next to the Palu Bay are severely damaged or lost due to the combined impact of tsunami and earthquake [1].

There are 5 buildings and supporting educational facilities destroyed and severely damaged or lost due to the combined impact of tsunami and earthquake as shown in Fig. 1 and Fig. 2. Of the total floor area, some 40% was moderately or severely damaged.

The principal objective of the subproject is to restore and improve UIN Datokarama's capacity to deliver tertiary-level education through the reconstruction of UIN Datokarama - Campus I based on disaster-resilient standards and with gender-responsive and inclusive features.

The masterplan considered the limited space available at the campus which has a total area of 2.6 ha. Reconstruction at another location was considered not feasible as the objective of an integrated campus would not be retained and would also require time-consuming and costly land acquisition. With part of the campus area falling within the "red" zone, which prohibits building construction in view of the tsunami risk, the possibility to explore design alternatives within the campus area were limited. Furthermore, a building design with more than four floors (ground floor included) could not be considered in view of the Paly City building regulations. While considering the spatial and building height limitations, a small part of the designed lecture and auditorium buildings fall within the red zone. This was considered acceptable in view of mitigation measures that will be taken to reduce the tsunami risk to the campus.

The building disaster-resilient design considered the tsunami and earthquake/ liquefaction risks. To mitigate the tsunami risk, the buildings have been designed with open space at the ground floor which will function as common area or parking place; brick walls will not be constructed on this floor. Furthermore, the new buildings are located away from the Palu Bay with the green zone between the buildings and the Bay as a buffer zone. The layout can be seen in Fig 3. As part of the disaster preparedness and response plan, two main building have been designed to also function as temporary shelter areas. The four-story lecture building includes shelter areas on the third and fourth floor with a total area of 833.25 m^2 which is accessible by staircases as well as an outside ramp facilitating access for people with disabilities. The three-story student center building provides a tsunami shelter area of 696 m^2 at its rooftop and connected to the lecture building at each floor. To mitigate the earthquake/ liquefaction risk,

*Corresponding author: azmimulki@mail.ugm.ac.id

the final design has adopted pile foundation for the buildings with a depth of 30 meter based on the result of Site-Specific Response Analysis (SSRA).

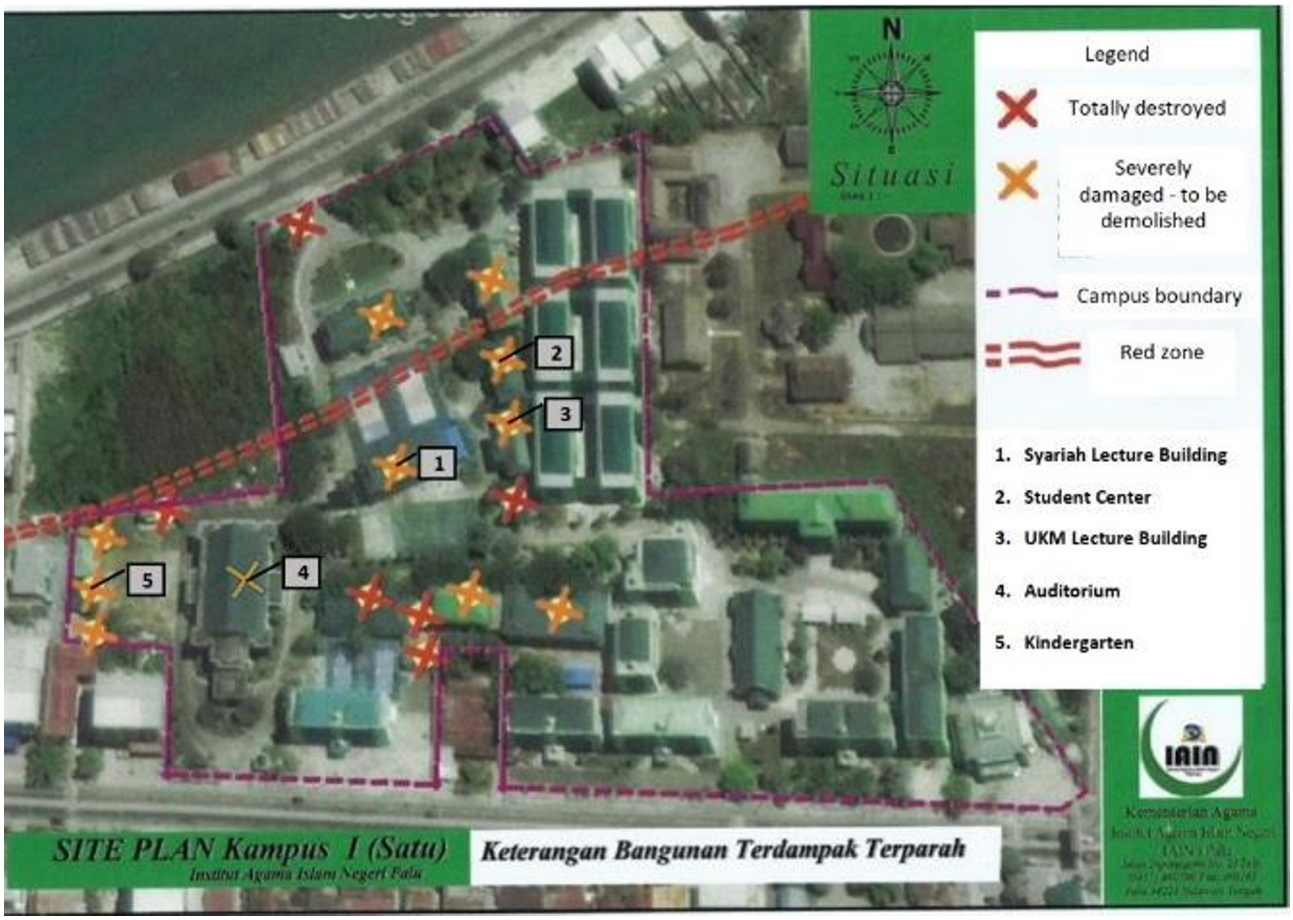

Fig. 1. Overview of destroyed and severely damaged buildings at IAIN's campus 1 [1].

Fig. 2. Examples of severely damaged buildings at IAIN's campus 1 [1].

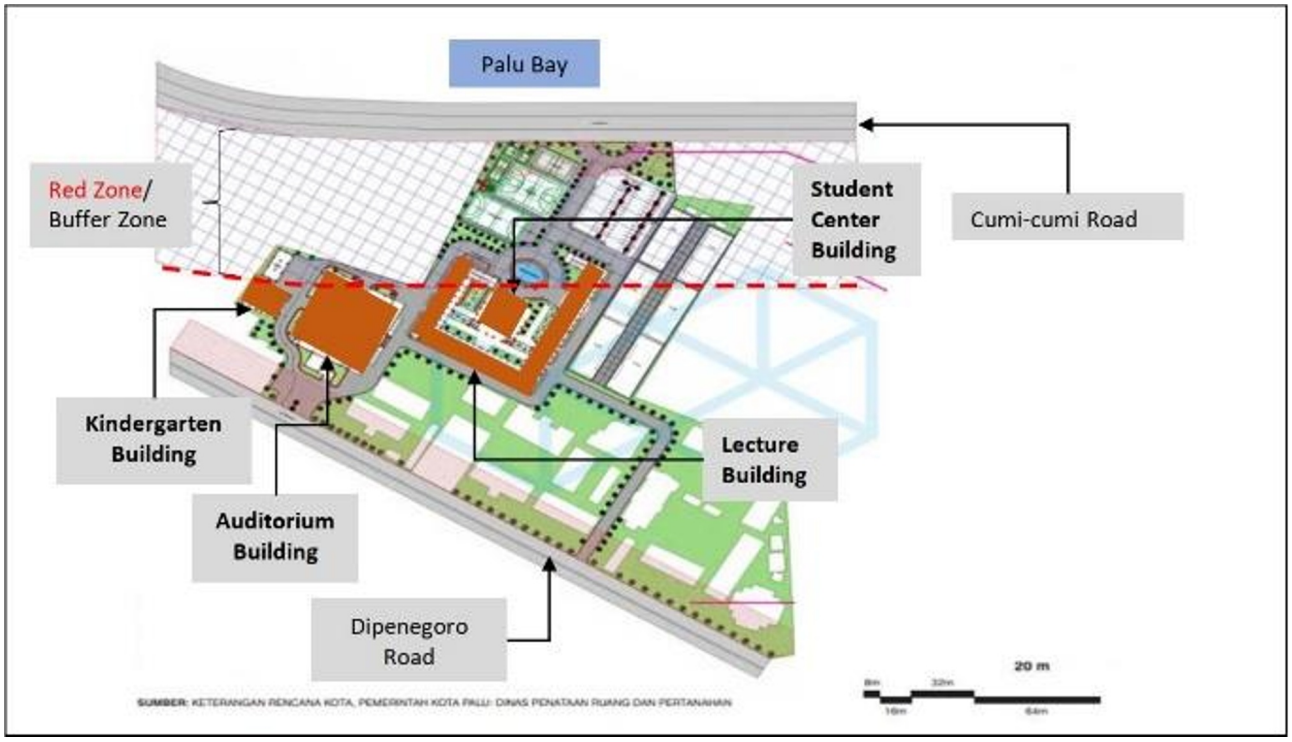

Fig 3. Layout plan for UIN Datokarama reconstruction [1].

2 Liquefaction potential hazard analysis

2.1 Liquefaction

Liquefaction takes place as earthquake shaking causes stresses and deformation in the ground, disrupting the soil structure of saturated loose granular soils. During shaking, contacts between soil grains are disrupted and become lose, dynamic loads previously carried through particle-to-particle contacts are transferred to the pore water. This will raise porewater pressure. When rising porewater pressure climbs to the level of the initial effective stress, soil effective stress reduces to zero and soil will behave from firm solid state to viscous liquid state. This sequence of events is known as liquefaction triggering.

2.2 Liquefaction prediction and assessment based on grain size

The grain size of each soil layer is analyzed and categorized based on Fig. 4 and further classified using the uniformity coefficient [3].

The uniformity coefficient, denoted as U_c, is calculated as the ratio of D_{60} (diameter of 60% finer) to D_{10} (diameter of 10% finer) and is standardized to a value of D_{60}/D_{10} =3.5. D_{10}, also known as effective size, is an important parameter for counting hydraulic conductivity and soil drainage [4]. A soil layer is considered non-liquefiable if its grain size accumulation curve does not fall within the possibility of liquefaction range.

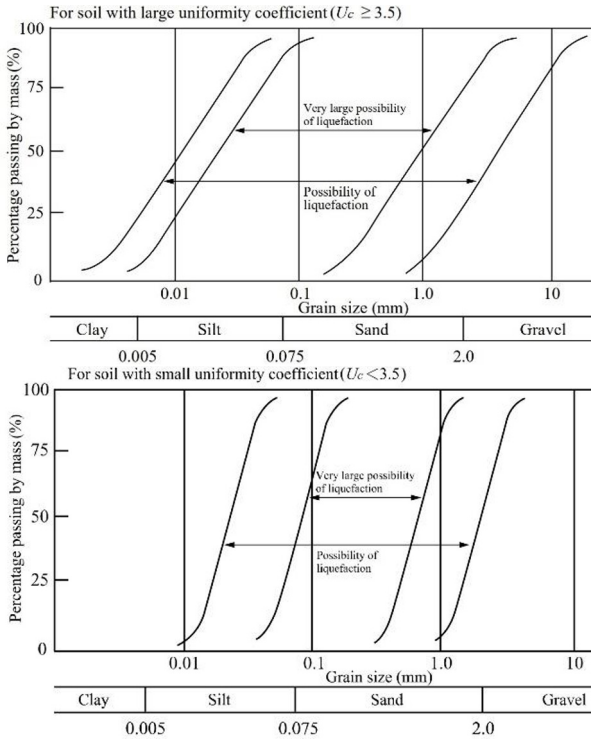

Fig 4. Range of possible liquefaction ($U_c \geq 3.5$ and $U_c < 3.5$).

2.3 Liquefaction triggering potential by stress-based approach

A stress-based method for assessing the potential of liquefaction triggering is done by comparing the earthquake-induced cyclic stress ratios (CSR) with the cyclic resistance ratios (CRR) of the soil [5-6]. To achieve that, factor of safety against soil liquefaction is recommended using an empirical procedure, which written as Equation 1.

$$FS_{liq} = \frac{CRR}{CSR} \quad (1)$$

where FS_{liq} = factor of safety against triggering of liquefaction.

Equation 2, the earthquake-triggered cyclic stress ratio (CSR) within the soil profile at a specific depth, denoted as z, is commonly represented as a single value, also known as the equivalent uniform value equal to 65% of the maximum cyclic shear stress ratio. where τ_{max} = maximum earthquake induced shear stress, σ_v' = vertical effective stress.

$$CSR = 0.65 \left(\frac{\tau_{max}}{\sigma_v'}\right) \quad (2)$$

The τ_{max} can be estimated using the Seed-Idriss simplified liquefaction procedure, so Equation 2 can will be written as Equation 3.

$$CSR = 0.65 \left(\frac{\sigma_v}{\sigma_v'}\right)\left(\frac{a_{max}}{g}\right) r_d \quad (3)$$

with σ_v = vertical total stress at depth z, a_{max}/g = maximum horizontal acceleration (as a fraction of gravity) at the ground surface, and r_d = shear stress reduction coefficient that accounts for dynamic/nonrigid response from the soil column.

r_d depends on magnitude of earthquake and depth, so the following Equations 4-6 will be used.

$$r_d = \exp[\alpha(z) + \beta(z).M] \quad (4)$$

$$\alpha(z) = -1{,}012 - 1.126 \sin\left(\frac{z}{11.73} + 5.133\right) \quad (5)$$

$$\beta(z) = 0.106 + 0.118 \sin\left(\frac{z}{11.28} + 5.142\right) \quad (6)$$

where z = depth below the ground surface in meters, and M = earthquake magnitude in moment magnitude (M_w).

Next, CRR will be calculated. CRR is evaluated to an in-situ parameter such as SPT blow count of the soil that is influenced by multiple procedural correction factors, including rod lengths, hammer energy, sampler details, borehole size, and by effective overburden stress. Thus, the correlation to CRR is based on corrected penetration resistance (Equations 7-8).

$$(N_1)_{60} = C_N C_E C_B C_R C_S N_m \quad (7)$$

$$C_N = \left(\frac{P_a}{\sigma_v'}\right)^{0.784 - 0.0768\sqrt{(N_1)_{60}}} \leq 1.7 \quad (8)$$

C_N is correction factor for overburden stress at 1 atm, P_a is atmospheric pressure equals to 101 kPa, C_E equals $ER_m/60\%$, where ER_m is the measured kinetic energy as a percentage of the theoretical free-fall hammer energy, C_R is a rod correction factor to account for energy ratios being smaller with shorter rod lengths, C_B is a correction factor for nonstandard borehole diameters, C_S is a correction factor for using split spoons with room for liners but is used with the liners absent, and N_m is the measured SPT blow count. All correction factors range values can be found in [6].

The fines content of soil (FC) influences the correlation of CRR to $(N_1)_{60}$. This correlation is represented in terms of equivalent clean sand $(N_1)_{60cs}$, which can be derived using the following formula Equations 9-10.

$$(N_1)_{60cs} = (N_1)_{60} + \Delta(N_1)_{60} \quad (9)$$

$$\Delta(N_1)_{60} = \exp\left(1.63 + \frac{9.7}{FC + 0.01} - \left(\frac{15.7}{FC + 0.01}\right)^2\right) \quad (10)$$

with FC in percent.

Effective overburden stress, which is quantified by a K_σ factor, and duration of earthquake shaking related to earthquake magnitude, which is correlated to MSF (Magnitude Scaling Factor), both have an impact on CRR. In order to adjust the correlation for CRR to other values of M and σ_v', the following Equation 11 is created for a reference M = 7.5 and σ_v' = 1 atm.

$$CRR = CRR_{M=7.5,\sigma_v'=1\ atm}\ MSF\ K_\sigma \quad (11)$$

$CRR_{M=7.5,\ \sigma v'=1\ atm}$ is CRR adjusted to M = 7.5 and σ_v' = 1 atm. It can be expressed in $(N_1)_{60cs}$ as Equation 12.

$$CRR_{M=7.5,\sigma'_{vc}=1\ atm} = exp\left(\frac{(N_1)_{60cs}}{14.1} + \left(\frac{(N_1)_{60cs}}{126}\right)^2 - \left(\frac{(N_1)_{60cs}}{23.6}\right)^3 + \left(\frac{(N_1)_{60cs}}{25.4}\right)^4 - 2.8\right) \quad (12)$$

The magnitude scaling factor (MSF) is utilized to approximately account for how the characteristics of the irregular cyclic loading produced by different magnitude earthquakes affect the potential for triggering of liquefaction [7]. The MSF relationship was derived by combining laboratory-based relationships between the CRR and the number of equivalent uniform loading cycles, and correlations of the number of equivalent uniform loading cycles with earthquake magnitude. The MSF values is evaluated in [5-6], using recommended Equation 13 which depended only on earthquake magnitude.

$$MSF = 6.9\ exp\left(\frac{-M}{4}\right) - 0.05 \leq 1.8 \quad (13)$$

Boulanger and Idriss revise the older MSF relationship [7]. The new MSF relationship relies on the soil characteristics as well as on earthquake magnitude instead of earthquake magnitude only. Equation 13 is revised as Equations 14-15.

$$MSF_{max} = 1.09 + \left(\frac{(N_1)_{60cs}}{31.5}\right)^2 \leq 2.2 \quad (14)$$

$$MSF = 1 + (MSF_{max} - 1)\left(8{,}64\ exp\left(\frac{-M}{4}\right) - 1.325\right) \quad (15)$$

where MSF_{max} is MSF's highest value for a minor magnitude earthquake relates to the case where the earthquake motion is predominantly a single strong acceleration pulse.

K_σ as overburden correction factor is computed in terms of the $(N_1)_{60cs}$ as Equations 16-17.

$$K_\sigma = 1 - C_\sigma \ln\left(\frac{\sigma'_v}{P_a}\right) \leq 1.1 \quad (16)$$

$$C_\sigma = \frac{1}{18.9 - 2.55\sqrt{(N_1)_{60cs}}} \leq 0.3 \quad (17)$$

2.4 Liquefaction potential index (LPI)

The Liquefaction Potential Index (LPI) indices are designed to offer a measure of the severity of surface manifestations based on the profile's cumulative liquefaction response.

The LPI [8] provides a depth-weighted index of the potential for triggering of liquefaction at a site. LPI is computed as Equation 18.

$$LPI = \int_0^{20} F\, w(z)\, dz \quad (18)$$

F = 1 – (FS_{liq}) for $FS_{liq} \leq 1$ and F = 0 for $FS_{liq} > 1$ (FS_{liq} is the factor of safety against liquefaction, obtained from liquefaction triggering potential by stress-based approach. w(z) is a linear depth weighting function given by w(z) = 10 – 0.5z (z is depth in meters below the ground surface) and w(z) = 0 for z > 20 m.

As a result, the resulting index is determined by the thickness of liquefiable layers in the uppermost 20 meters, their proximity to the ground surface, and the amount by which the FS against liquefaction is less than 1.0. The LPI is applicable to a profile that contains numerous liquefiable layers. LPI can vary from 0 (no layers with an FS less than 1 in the top 20 meters of soil) to 100 (the FS against liquefaction is zero for all layers in the uppermost 20 meters). Data from 45 liquefied sites in Niigata, Japan, were analysed, and it was discovered that severe liquefaction occurred at sites with LPI greater than 15, and minor liquefaction occurred at locations with LPI less than 5. See Table 1 for full risk level.

Table 1. Liquefaction severity level based on LPI.

LPI	Liquefaction severity level
LPI = 0	Liquefaction risk is very low
0 < LPI ≤ 5	Liquefaction risk is low
5 < LPI ≤ 15	Liquefaction risk is high
LPI > 15	Liquefaction risk is very high

3 Method and analysis

3.1 Data

The research area is located at the UIN Datokarama reconstruction site. The soil properties and SPT used in this study are taken from 6 borelogs and laboratory test results. Fig. 5 shows the locations of the six borelogs and Tables 2-3 shows the soil profile from each borelogs. Coordinate for each borelogs are BH-01 (0°53'4.22"S 119°50'40.56"E), BH-02 (0°53'3.83"S 119°50'41.85"E), BH-03 (0°53'5.19"S 119°50'43.85"E), BH-04 (0°53'5.17"S 119°50'43.93"E), BH-05 (0°54'31.37"S, 119°52'33.64"E), DB-01 (0°53'3.7962"S 119°50'43.494"E).

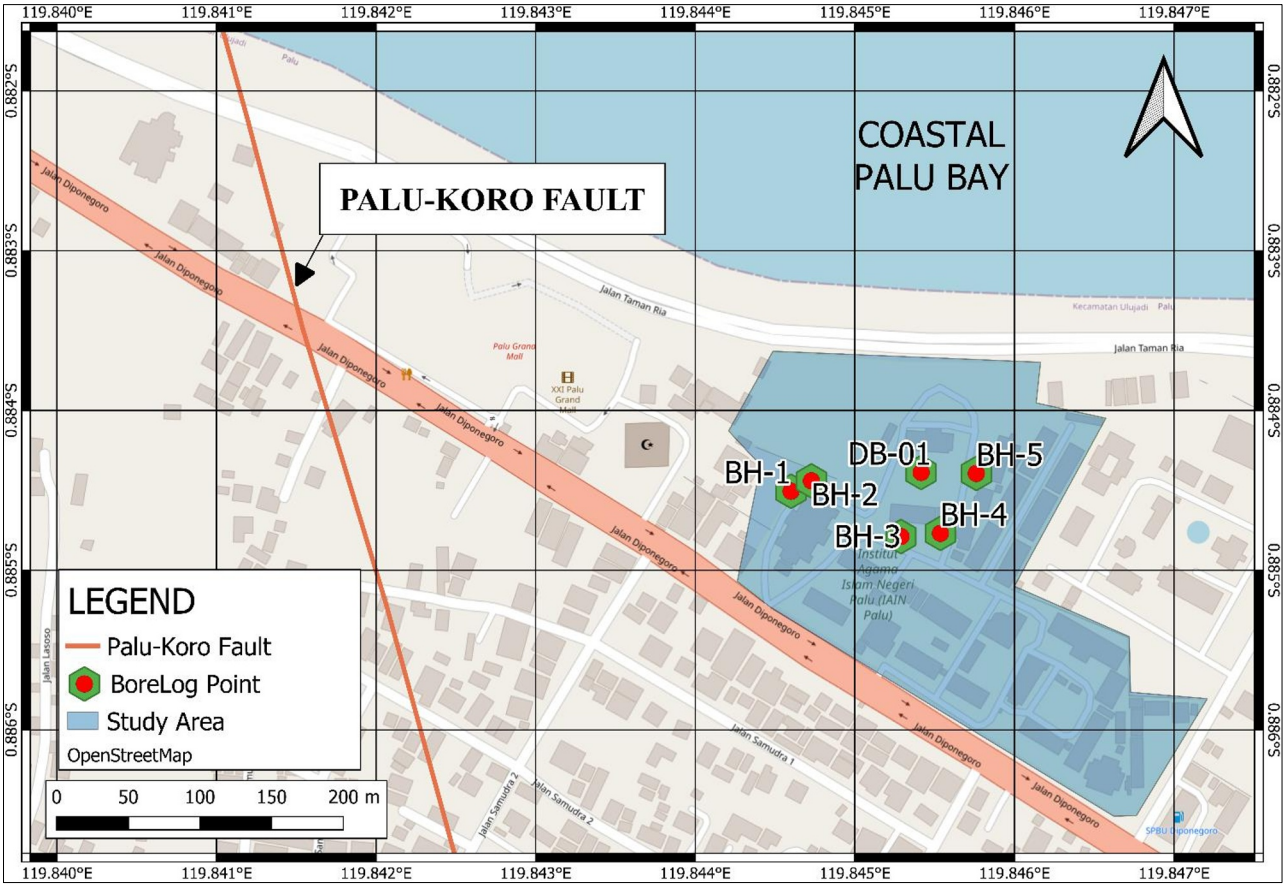

Fig. 5. Borelog and research area map (basemap sources: openstreetmap, freely licensed under open database license.

Table 2. Soil profile.

Depth (m)	BH-01			BH-02			BH-03		
	N	Soil Type (USCS)	Density / Consistency	N	Soil Type (USCS)	Density / Consistency	N	Soil Type (USCS)	Density / Consistency
2	4	SP	Very Loose	7	SC-SM	Loose	11	SP	Medium
4	5	SP	Loose	12	SC-SM	Medium	9	SP	Loose
6	9	SM	Loose	14	SP-SM	Medium	6	SP	Loose
8	5	SM	Loose	14	SP-SM	Medium	7	SP	Loose
10	8	SM	Loose	10	SP-SM	Loose	10	SP	Loose
12	5	SP	Loose	11	SM	Medium	13	SP	Medium
14	4	SP	Very Loose	11	SM	Medium	13	SP	Medium
16	7	SM	Loose	15	SM	Medium	13	SP	Medium
18	39	SM	Dense	15	SM	Medium	13	SP	Medium
20	42	SM	Dense	29	SM	Medium	12	SP	Medium
22	43	SC	Dense	24	SP	Medium	8	SP	Loose
24	43	SC	Dense	27	SP	Medium	6	SP	Loose
26	46	SC	Dense	29	SC	Medium	4	SP	Very Loose
28	48	SC	Dense	29	SC	Medium	11	SP	Medium
30	61	SC	Very Dense	37	SC	Dense	12	SP	Medium

Table 3. Soil profile (continued).

Depth (m)	BH-04			BH-05			BH-06		
	N	Soil Type (USCS)	Density / Consistency	N	Soil Type (USCS)	Density / Consistency	N	Soil Type (USCS)	Density / Consistency
2	6	SP	Loose	6	SP	Loose			
4	7	SP	Loose	7	SP	Loose	14	SP-SM	Medium
6	6	SP	Loose	11	SP	Medium	14	SP	Medium
8	7	SP	Loose	11	SP	Medium	6	SM	Loose
10	7	SP	Loose	12	SP	Medium	10	SP	Loose
12	6	SP	Loose	10	SP	Loose	16	SP	Medium
14	7	SP	Loose	10	SP	Loose	13	SM	Medium
16	5	SP	Loose	10	SP	Loose	14	SC	Medium
18	5	SP	Loose	10	SP	Loose	15	CL	Stiff
20	19	SP	Medium	11	SP	Medium	14	CL	Stiff
22	20	SP	Medium	18	SP	Medium	13	CL	Stiff
24	20	SP	Medium	15	SP	Medium	14	CL	Stiff
26	4	SP	Very Loose	4	SP	Very Loose	14	CL	Stiff
28	9	SP	Loose	35	SP	Dense	15	CL	Stiff
30	10	SP	Loose	28	SP	Medium	50	CL	Hard

Input parameters is taken from [1]. Peak ground acceleration (g) = 0.43 g, earthquake magnitude M_w=7.5, w, and groundwater depth = 1.2 m.

3.2 Liquefaction triggering potential analysis based on grain size

Most of the soil at the study site is saturated sandy soil with relative density loose to medium. Soils with relative density dense to very dense are only found in BH-01 at a depth of 18 to 30 meters. Clay soil is only found in DB-01 with stiff to hard consistency at the same depth of 18 to 30 meters.

The grain size distribution from each soil layer is checked whether or not the soil falls within the range of possible liquefaction.

3.3 Liquefaction triggering potential analysis

The Equations 1-17 is used to compute the liquefaction triggering potential, the parameters is taken from [1-2]. The result is expressed in factor of safety against soil liquefaction, FS_{liq}, with $FS_{liq} < 1$ = liquified (L) (Tables 4-5).

The situation is further aggravated by all boreholes having LPI > 15, which means that the damage from liquefaction to the reconstruction site will be at very high risk level. More measurable mitigation efforts are needed to deal with this, such as by using deep foundations that penetrate deep soil layers that are not liquefied.

3.4 Liquefaction potential index (LPI) analysis

LPI analysis use Equation 18 to calculate the severity of liquefaction to structures above ground (Table 6).

Table 4. Liquefaction triggering potential analysis.

D	BH-01				BH-02				BH-03			
(m)	**CSR**	**CRR**	**FOS**	**(L/NL)**	**CSR**	**CRR**	**FOS**	**(L/NL)**	**CSR**	**CRR**	**FOS**	**(L/NL)**
2	0.36	0.11	0.29	L	0.35	0.20	0.55	L	0.35	0.21	0.60	L
4	0.45	0.12	0.26	L	0.43	0.27	0.64	L	0.42	0.16	0.37	L
6	0.47	0.20	0.42	L	0.45	0.22	0.48	L	0.45	0.11	0.25	L
8	0.48	0.13	0.28	L	0.46	0.19	0.41	L	0.46	0.11	0.25	L
10	0.47	0.16	0.33	L	0.45	0.13	0.29	L	0.46	0.13	0.29	L
12	0.46	0.09	0.19	L	0.45	0.18	0.39	L	0.45	0.15	0.34	L
14	0.45	0.08	0.18	L	0.44	0.16	0.38	L	0.44	0.14	0.32	L
16	0.44	0.13	0.30	L	0.42	0.17	0.39	L	0.43	0.16	0.38	L
18	0.42	1.68	2.00	-	0.41	0.16	0.38	L	0.41	0.15	0.37	L
20	0.41	1.60	2.00	-	0.40	0.42	1.07	-	0.40	0.14	0.35	L
22	0.39	1.54	2.00	-	0.38	0.20	0.51	L	0.39	0.10	0.26	L
24	0.38	1.48	2.00	-	0.37	0.22	0.59	L	0.38	0.09	0.24	L
26	0.36	1.43	2.00	-	0.36	0.32	0.91	L	0.37	0.07	0.19	L
28	0.35	1.38	2.00	-	0.35	0.29	0.84	L	0.36	0.09	0.26	L
30	0.34	1.34	2.00	-	0.34	0.79	2.00	-	0.35	0.10	0.27	L

Table 5. Liquefaction triggering potential analysis (continued).

D	BH-04				BH-05				DB-01			
(m)	**CSR**	**CRR**	**FOS**	**(L/NL)**	**CSR**	**CRR**	**FOS**	**(L/NL)**	**CSR**	**CRR**	**FOS**	**(L/NL)**
2	0.35	0.13	0.37	L	0.35	0.15	0.44	L				
4	0.43	0.14	0.31	L	0.43	0.16	0.37	L	0.42	0.24	0.56	L
6	0.46	0.12	0.25	L	0.46	0.17	0.38	L	0.44	0.21	0.47	L
8	0.47	0.12	0.25	L	0.46	0.15	0.33	L	0.45	0.14	0.31	L
10	0.47	0.11	0.24	L	0.46	0.15	0.34	L	0.45	0.13	0.29	L
12	0.46	0.10	0.21	L	0.45	0.15	0.33	L	0.44	0.18	0.40	L
14	0.45	0.10	0.22	L	0.44	0.14	0.32	L	0.43	0.19	0.43	L
16	0.44	0.08	0.19	L	0.43	0.11	0.26	L	0.42	0.18	0.43	L
18	0.42	0.08	0.19	L	0.41	0.11	0.25	L	na	na	na	na
20	0.41	0.17	0.40	L	0.40	0.11	0.27	L	na	na	na	na
22	0.40	0.16	0.42	L	0.39	0.15	0.37	L	na	na	na	na
24	0.38	0.16	0.41	L	0.38	0.12	0.32	L	na	na	na	na
26	0.37	0.07	0.19	L	0.37	0.07	0.19	L	na	na	na	na
28	0.36	0.09	0.24	L	0.35	0.39	1.10	-	na	na	na	na
30	0.35	0.09	0.25	L	0.34	0.19	0.56	L	na	na	na	na

Table 6. LPI.

Borehole	LPI
BH-01	68
BH-02	52.69
BH-03	63.06
BH-04	72.38
BH-05	63.89
DB-01	52.47

4 Conclusion

The UIN Datokarama Palu reconstruction site primarily consists of saturated sandy soil with a very shallow groundwater level 1.2 m from the ground surface. Cohesive soils are only found in borehole DB-01.

From the stress-based analysis of liquefaction triggering potential, liquefaction occurred in all boreholes at various depths. The most extreme conditions are found at BH-02, BH-03, and BH-05, where almost all soil layers are potentially liquefied.

References

1. Directorate General of Human Settlement Ministry of Public Works and Housing, Summary subproject report for the rehabilitation of the islamic university, Palu, Central Sulawesi, (2020)
2. PT Geotechnical Engineering Consultant, Seismic hazard study & site-specific response analysis (SSRA) IAIN Palu final report – Rev 01 (2020)
3. The Committee for Propagating Japanese Technical Standards Abroad, Technical standards and commentaries for port and harbour facilities in Japan (The Overseas Coastal Area Development Institute of Japan, 2020)
4. B.M. Das, K. Sobhan, Principles of geotechnical engineering 9th Ed. (Cengage Learning, 2018)
5. I.M Idriss, R.W. Boulanger, SPT-based liquefaction triggering procedures (Report No. UCD/CGM-10-02, University of California, 2010)

6. I.M Idriss, R.W. Boulanger, Soil liquefaction during earthquakes (Earthquake Engineering Research Institute, 2008)
7. R.W. Boulanger, I.M Idriss, Soil Dynamics and Earthquake Engineering **79**(B), 296-303 (2015) https://doi.org/10.1016/j.soildyn.2015.01.004
8. T. Iwasaki, T. Arakawa, K. Tokida, International Journal of Soil Dynamics and Earthquake Engineering **3**(1), 49-58 (1984) https://doi.org/10.1016/0261-7277(84)90027-5